

## Predicting Linear Operating Range for Charged Aerosol Detection Using an Inverse Power Function Framework

---

Robert Birdsall, Xiangsha Du, Pawel Bigos, Duanduan Han, Jennifer Simeone, Nikhil Bhiwankar

Waters Corporation, United States

Published on June 15, 2026

For research use only. Not for use in diagnostic procedures.

Main

*For research use only. Not for use in diagnostic procedures.*

---

### Abstract

Liquid chromatography (LC) coupled with charged aerosol detection (CAD) is widely used for quantitative analysis of compounds that lack strong chromophores, including lipids, surfactants, carbohydrates, and small molecule impurities. As a universal, mass-dependent detector, CAD enables detection of analytically challenging analytes; however, detector response is inherently non-linear as a result of aerosol formation and detection properties. To address this behavior, CAD instruments provide an adjustable power function value (PFV) setting that effectively extends the linear response range during data acquisition.

Traditionally, selection of PFV settings has relied on empirical trial-and-error experimentation requiring multiple calibration curves and repeated injections. This application note presents a model-based approach that uses calibration data acquired at a single reference condition (PFV = 1.00) to characterize intrinsic detector response and to predict operating PFV ranges that provide linear behavior. Using an inverse power function

framework, detector response is simulated forward to define confidence-based working ranges.

This data-driven strategy enables objective optimization of CAD settings during method development and can be readily adapted to manufacturing environments. The approach reduces experimental burden while improving quantitative robustness and consistency.

## Benefits

- Accelerated method development with reduced experimental trial-and-error burden
- Objective definition of linear operating range through variance-based modeling and residual analysis
- Improved quantitative robustness by aligning detector scaling, working range, and regression strategy
- Compliant-ready workflow compatibility using standard calibration data and statistical tools within the Empower™ Chromatography Data System (CDS)

---

## Introduction

Universal aerosol-based detectors are widely employed for quantitative LC analysis of compounds that lack strong chromophores, including lipids, surfactants, carbohydrates, and selected small molecule impurities.<sup>1-5</sup> Their broad applicability and mass-dependent response make these detectors well suited for pharmaceutical research, method development, and quality control applications. However, detector response for aerosol-based techniques is inherently non-linear with respect to analyte amount due to aerosol formation, particle size distribution, and properties intrinsic to detector operation.<sup>6</sup>

To manage this non-linear behavior, CAD instruments provide user-defined response scaling parameters, such as PFV, that can be applied during data acquisition to extend the effective linear response range. In practice, selection of PFV settings is commonly performed empirically by evaluating calibration performance across multiple detector settings. While this approach is widely used, it can require repeated experimental iterations and does not inherently provide insight into the relationship between detector scaling, quantitative uncertainty, and usable working range.

This application note describes a model-based, data-driven approach for optimizing CAD response using an inverse power function framework. Calibration data acquired at a single reference setting (PFV = 1.00) is used to characterize intrinsic detector response behavior and to predict the effective linear operating range at alternative PFV settings. This strategy supports objective selection of detector parameters expediting method development and deployment in manufacturing environments.

---

## Experimental

All lipids in this study were used for research and demonstration purposes and were purchased from the following vendors: cholesterol and DSPC from Sigma-Aldrich; DMG-PEG 2000 and SM-102 from Cayman Chemical. Stocks of each lipid were prepared in methanol at 5 mg/mL and diluted to the appropriate concentration at 90/10 water/methanol (v/v). Data acquisition and analysis was performed in Empower CDS and Microsoft® Excel® Software.

|                          |   |
|--------------------------|---|
| LC system:               | ACQUITY™ Premier System (BSM)   |
| Detection:               | TUV, $\lambda = 200 / 280$ nm<br>FC = 5mm Ti, 1Hz, time constant = normal   |
| Column:                  | Waters GTxResolve™ Lipid Phenyl-Hexyl+ RP Column, MaxPeak™ Premier Technology, SPP, 1.6 $\mu$ m, 230Å, 2.1 x 50 mm (p/n: 186011698) |
| Column temperature:      | 50 °C   |
| Sample temperature:      | Ambient   |
| Injection volume:        | 3 $\mu$ L   |
| Flow rate:               | 0.400 mL/min  |
| Mobile phase:            | A: 0.1% formic acid in water<br>B: 50:50 MeOH:MeCN, 0.1% formic acid  |
| Chromatography software: | Empower CDS   |

CAD settings

---

|                          |        |
|--------------------------|--------|
| Sampling rate:           | 10 Hz  |
| Time constant:           | Normal |
| Ion trap:                | 20 V   |
| Evaporation temperature: | 35 °C  |

## Gradient Table

| Time (min) | Flow (mL/min) | %A   | %B   | Curve   |
|------------|---------------|------|------|---------|
| Initial    | 0.400         | 50.0 | 50.0 | initial |
| 6.00       | 0.400         | 10.0 | 90.0 | 6       |
| 8.00       | 0.400         | 10.0 | 90.0 | 6       |
| 8.50       | 0.400         | 50.0 | 50.0 | 6       |
| 12.00      | 0.400         | 50.0 | 50.0 | 6       |

---

## Results and Discussion

### Intrinsic CAD Response Behavior

The response of a CAD can be described by a power law relationship, in which detector signal is proportional to analyte amount raised to an exponential term. When calibration data acquired at PFV = 1.00 are assessed on linear axes, this relationship results in a characteristic non-linear response across wide concentration ranges (Figure 1A, blue curve). This curvature reflects the intrinsic behavior of the detector rather than experimental artifacts. The PFV, described as the reciprocal of the exponent term of the power law response curve, serves as a correction factor during acquisition.<sup>5</sup> By optimizing this setting, CAD response can be transformed such that the effective exponent term in the response curve approaches a value of 1.0 resulting in a linearized response over a defined operating range.

As shown in Figure 1A, the inverse power function provides a mathematical basis in determining a linear operating range post-acquisition. The exponent term describing intrinsic detector response is preserved wherein an optimal PFV (*i.e.*  $1/p$ ) can be estimated directly from PFV = 1.00 calibration data, enabling predictive modeling without modification of raw analytical results. An example of this approach is shown in Figure 1B, where calibration data acquired at PFV = 1.00 can be modeled using ordinary least squares regression to estimate the intrinsic response exponent necessary to achieve a linear response (Figure 1C).

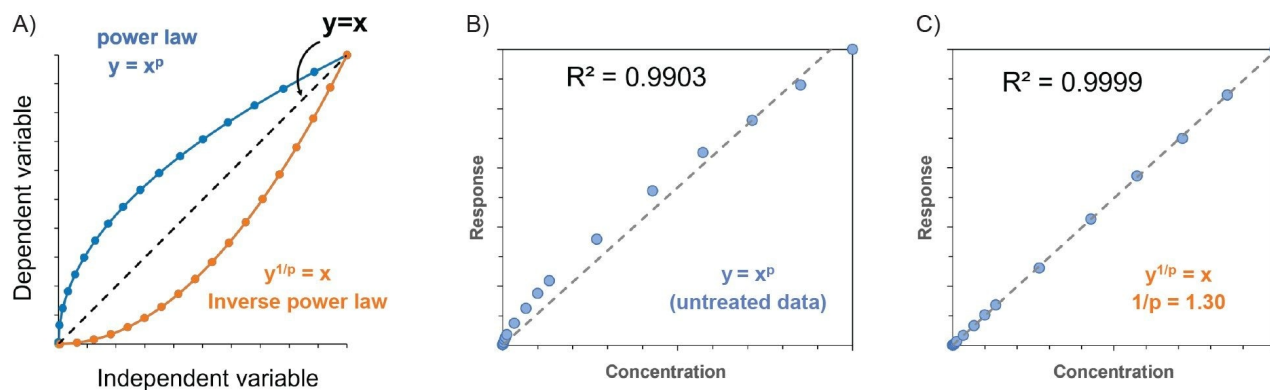


Figure 1. A) Generalized representation of CAD response following a power-law relationship. B) Intrinsic nonlinear CAD response acquired at PFV = 1.00, where detector signal increases as a function of analyte amount raised to an exponent  $p$  (untreated data). C) An example of linearization of the same calibration curve using an inverse power function transformation  $1/p = 1.30$ , illustrating how appropriate selection of PFV mathematically corrects detector nonlinearity and enables definition of an effective linear operating range without altering the underlying analytical data.

## Predictive Modeling Using PFV = 1.00 Calibration Data

While Figure 1 establishes the theoretical basis for correcting intrinsic CAD nonlinearity using an inverse power function, practical application requires translating this relationship into a quantitative framework that can operate directly on experimental calibration data. To achieve this, PFV = 1.00 calibration data were modeled using standard regression techniques to estimate the intrinsic response exponent and forward-simulate detector behavior across alternate PFV settings.

This predictive modeling framework enables objective estimation of expected linearity, deviation, and usable working range at different PFVs without acquiring additional experimental calibration data. The approach allows detector settings to be evaluated systematically using standard regression metrics rather than empirical trial-and-error experimentation, improving efficiency and robustness during method development.

Implementation of this framework can be deployed using commonly available statistical tools. An example of a globally accessible implementation using Microsoft Excel Software is shown in Figure 2, where model-derived metrics including coefficient of determination ( $R^2$ ), residual behavior, and weighting effects, are dynamically linked to a user-defined PFV setting. These metrics are presented both numerically for the current PFV under evaluation and visually across a continuous PFV sweep representing instrument range from 0.60 to 2.00, supporting global assessment of detector operating conditions.

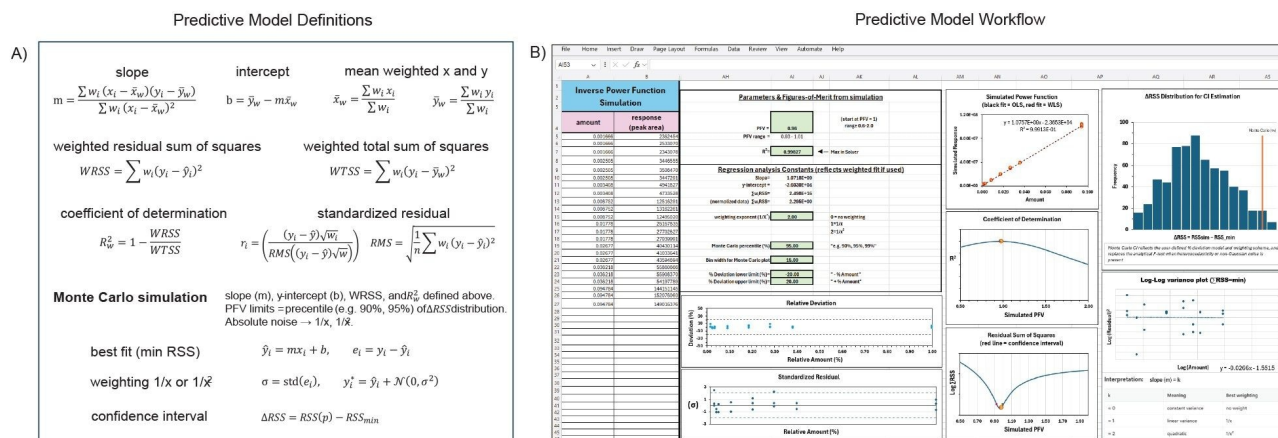


Figure 2. Predictive modeling framework used to characterize intrinsic CAD response and simulate detector behavior at alternative PFV settings using calibration data acquired at PFV=1.00. A) Statistical definitions shown include weighted least-squares regression parameters, coefficient of determination, residual metrics, and confidence interval criteria. B) The model enables forward simulation of detector response and objective evaluation of PFV-dependent linearity using standard spreadsheet-based tools such as Microsoft Excel Software. Contact your Waters representative for more information about the predictive modeling workflow.

## Application to a Representative Analytical System

Lipid nanoparticle (LNP) components were selected as a representative analytical system to demonstrate the utility of the inverse power function modeling approach (Figure 3). The formulation includes ionizable lipid (SM-102), cholesterol, phospholipid (DSPC), and PEGylated lipid (DMG-PEG2000), spanning a wide polarity and concentration range typical of LNP analysis. This chemical diversity provides a relevant and challenging test case for evaluating CAD linearity, dynamic range, and regression behavior.

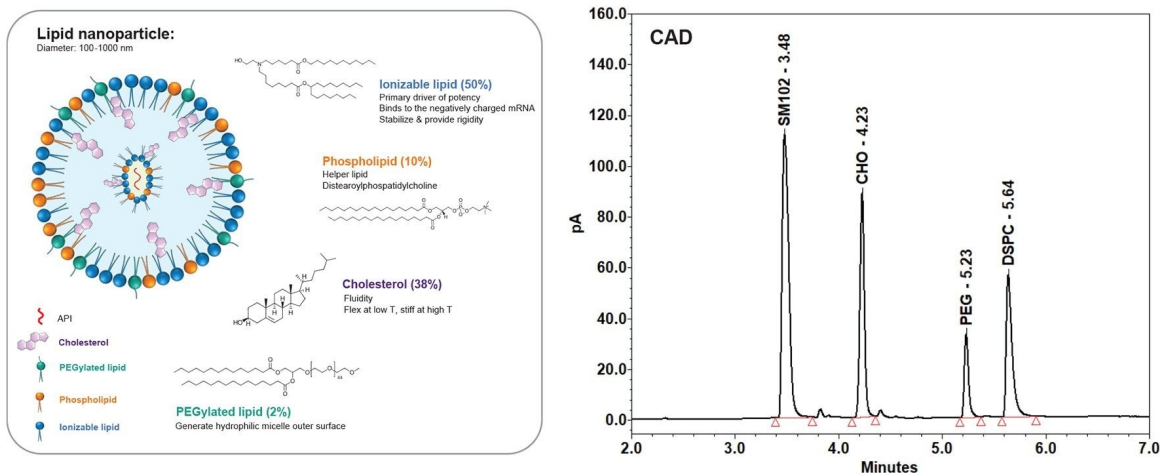


Figure 3. Representative LNP composition used to demonstrate inverse power function modeling of CAD response.

## Defining an Effective Linear Operating Range

To determine the effective linear response range for each lipid species, concentration and associated peak area for a calibration plot acquired at an instrument setting of PFV = 1.00 were imported into the model (column A and B). The  $R^2$  cell was “maximized” using the solver tool in the Microsoft Excel Software to change the PFV cell within a range of 0.60-2.00. Confidence intervals were assigned at 95% using Monte Carlo simulation with Gaussian noise derived from the residual standard deviation. This effectively provides a range of PFVs to evaluate during optimization. Using this approach, PFV settings ranging between 1.14-1.34 were identified as offering predictable linear response for the four LNP species. To test the accuracy of the model, experimental data was acquired at PFV = 1.30 and is shown in the tables of Figure 4. While correlation coefficients provide a useful initial assessment of calibration performance, evaluation of residual behavior offers additional insight into quantitative reliability.

Because CAD calibration data inherently exhibit heteroscedastic variance across wide dynamic ranges, predicted linearity must be evaluated not only through correlation metrics but also through residual behavior and appropriate regression weighting. Application of  $1/x$  and  $1/x^2$  weighting schemes improved accuracy relative to unweighted regression, as shown in Figure 4. To determine the most appropriate weighting strategy, standardized residuals were evaluated across all LNP species as a function of analyte amount. As shown in Figure 5, unweighted regression exhibited expanding residual variance across the calibration range, indicative of heteroscedasticity, while application of  $1/x^2$  weighting produced excessive compression of residuals, consistent with overweighting at lower concentrations. In contrast,  $1/x$  weighting resulted in approximately constant variance across the concentration range, with most residuals contained within  $\pm 2$  standardized deviation units and were therefore selected for comparative analysis.

These diagnostics support objective definition of an effective linear working range and inform appropriate selection of regression weighting strategies. This variance- and residual-based evaluation of linearity is consistent with the principles outlined in ICH Q2 for defining method linearity and range as well as provides a more informative basis for assessing quantitative performance than correlation metrics alone.<sup>6</sup>

| SM102                         |          |         |        |               |                  |               | Cholesterol                   |         |       |       |                  |               |          | DMG-PEG 2000                  |        |        |                  |               |          |         | DSPC                          |       |                  |      |               |  |  |
|-------------------------------|----------|---------|--------|---------------|------------------|---------------|-------------------------------|---------|-------|-------|------------------|---------------|----------|-------------------------------|--------|--------|------------------|---------------|----------|---------|-------------------------------|-------|------------------|------|---------------|--|--|
| Simulator PFV range 1.28–1.32 |          |         |        | Deviation (%) |                  |               | Simulator PFV range 1.14–1.29 |         |       |       | Deviation (%)    |               |          | Simulator PFV range 1.21–1.37 |        |        |                  | Deviation (%) |          |         | Simulator PFV range 1.20–1.29 |       |                  |      | Deviation (%) |  |  |
| Experimental PFV              |          |         | 1.30   | weighting     |                  |               | Experimental PFV              |         |       | 1.30  | weighting        |               |          | Experimental PFV              |        |        | 1.30             | weighting     |          |         | Experimental PFV              |       |                  | 1.30 | weighting     |  |  |
| conc. (mg/mL)                 | Area     | RSD (%) | none   | 1/x           | 1/x <sup>2</sup> | conc. (mg/mL) | Area                          | RSD (%) | none  | 1/x   | 1/x <sup>2</sup> | conc. (mg/mL) | Area     | RSD (%)                       | none   | 1/x    | 1/x <sup>2</sup> | conc. (mg/mL) | Area     | RSD (%) | none                          | 1/x   | 1/x <sup>2</sup> |      |               |  |  |
| 0.0043                        | 6.31E+06 | 4.19    | -69.84 | -12.25        | -2.23            | 0.0017        | 2.41E+06                      | 4.33    | 33.55 | 11.27 | 4.97             | 0.0004        | 1.17E+06 | 5.43                          | -43.18 | -15.84 | -8.40            | 0.0009        | 1.81E+06 | 19.29   | 14.63                         | 8.32  | 3.55             |      |               |  |  |
| 0.0065                        | 9.36E+06 | 3.58    | -42.40 | -5.62         | -0.56            | 0.0025        | 3.47E+06                      | 1.02    | 14.08 | -0.31 | -3.70            | 0.0006        | 1.62E+06 | 8.95                          | -19.74 | -2.41  | 1.18             | 0.0013        | 2.77E+06 | 2.84    | 8.32                          | 4.28  | 1.86             |      |               |  |  |
| 0.0089                        | 1.30E+07 | 1.68    | -24.50 | 1.18          | 3.47             | 0.0034        | 4.84E+06                      | 3.04    | 8.14  | -2.03 | -3.74            | 0.0008        | 2.29E+06 | 4.83                          | 4.71   | 16.54  | 17.72            | 0.0017        | 3.41E+06 | 2.63    | -4.78                         | -7.67 | -9.08            |      |               |  |  |
| 0.0230                        | 3.28E+07 | 0.93    | -0.89  | 6.26          | 4.17             | 0.0088        | 1.27E+07                      | 2.98    | -2.67 | -5.69 | -4.59            | 0.0021        | 4.24E+06 | 1.22                          | -6.62  | -3.04  | -4.27            | 0.0045        | 9.70E+06 | 4.64    | -2.55                         | -3.39 | -2.52            |      |               |  |  |
| 0.0467                        | 6.45E+07 | 1.97    | 3.64   | 4.92          | 1.54             | 0.0178        | 2.70E+07                      | 2.85    | -2.18 | -2.81 | -0.68            | 0.0042        | 8.24E+06 | 0.95                          | -1.10  | -0.39  | -2.69            | 0.0091        | 1.99E+07 | 4.12    | -4.00                         | -4.19 | -2.63            |      |               |  |  |
| 0.0704                        | 9.72E+07 | 0.65    | 6.47   | 5.78          | 1.92             | 0.0268        | 4.17E+07                      | 4.03    | -0.39 | -0.22 | 2.30             | 0.0063        | 1.27E+07 | 3.40                          | 5.22   | 4.91   | 2.12             | 0.0137        | 3.15E+07 | 1.81    | 0.12                          | 0.17  | 2.06             |      |               |  |  |
| 0.0952                        | 1.29E+08 | 2.22    | 5.74   | 4.12          | 0.12             | 0.0362        | 5.53E+07                      | 1.76    | -2.49 | -1.96 | 0.67             | 0.0086        | 1.67E+07 | 0.98                          | 3.20   | 2.47   | -0.41            | 0.0185        | 4.36E+07 | 3.15    | 2.11                          | 2.28  | 4.34             |      |               |  |  |
| 0.2492                        | 3.08E+08 | 1.03    | -1.39  | -4.39         | -8.41            | 0.0948        | 1.48E+08                      | 2.69    | 0.46  | 1.75  | 4.77             | 0.0225        | 4.08E+07 | 2.15                          | -0.77  | -2.23  | -5.24            | 0.0485        | 1.12E+08 | 0.23    | -0.16                         | 0.20  | 2.41             |      |               |  |  |

Figure 4. Experimental calibration results acquired at PFV=1.30 for four LNP components (SM-102, cholesterol, DMG-PEG2000, and DSPC). Tables summarize concentration, peak area, precision, and percent deviation from linear regression using unweighted,  $1/x$ , and  $1/x^2$  weighting schemes.

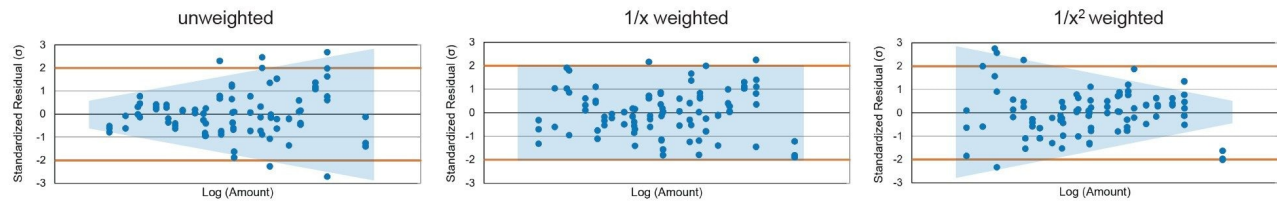


Figure 5. Standardized residual plots of all LNP species as a function of analyte amount (log-scale) illustrating the impact of regression weighting on variance behavior. Unweighted regression exhibits expansion of residuals at higher concentrations (heteroscedasticity), while  $1/x^2$  weighting results in over-compression. A  $1/x$  weighting scheme produces near-constant variance across the calibration range, supporting its selection for quantitative optimization. Shaded regions indicate visual variance envelopes.

## Comparison of Simulated and Experimental Performance

Regression statistics derived from experimentally acquired calibration data acquired at  $PFV = 1.30$  were compared to simulation raw data ( $PFV = 1.00$ ) using a simulator setting of  $1/p=1.30$ . Both data sets were evaluated with  $1/x$  weighting. As summarized in Figure 6A, experimental data was in good agreement with the simulation in terms of correlation factor and residual behavior. Notably, experimental data for all LNP species were within  $\leq 0.08$  of their optimal  $PFV$  when imported into the simulator, demonstrating the ability of the model to predict key experimental performance characteristics, including correlation coefficients, residual trends, and relative deviation across the calibration range (Figure 6B).

Collectively, these results demonstrate that inverse power function modeling based on  $PFV = 1.00$  calibration data provides an accurate representation of intrinsic CAD response behavior and can be used to inform detector configuration decisions.

A) **PFV 1.30 Data**

| figure of merit | SM102     |              | Cholesterol |              | DMG-PEG 2000 |              | DSPC      |              |
|-----------------|-----------|--------------|-------------|--------------|--------------|--------------|-----------|--------------|
| Data            | Simulated | Experimental | Simulated   | Experimental | Simulated    | Experimental | Simulated | Experimental |
| PFV             | 1.30      | 1.30         | 1.30        | 1.30         | 1.30         | 1.30         | 1.30      | 1.30         |
| R <sup>2</sup>  | 0.9997    | 0.9968       | 0.9972      | 0.9992       | 0.9980       | 0.9977       | 0.9964    | 0.9988       |
| ΣWRSS           | 0.0038    | 0.0511       | 0.1440      | 0.0522       | 0.3925       | 0.0477       | 0.3433    | 0.1213       |

B)

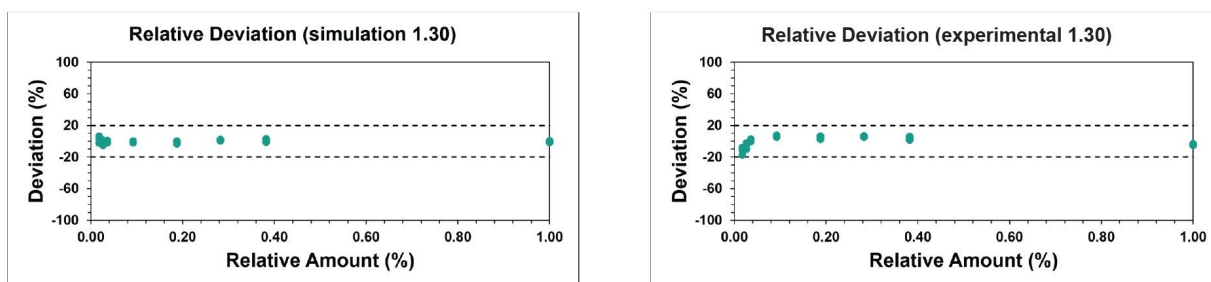


Figure 6. Comparison of simulated raw data (PFV=1.00) linearized with  $1/p=1.30$  and experimentally acquired data collected at PFV=1.30. (A) Regression statistics for simulated data and experimental data for each lipid component using  $1/x$  weighting and (B) visual comparison of relative deviation. Results demonstrate that PFV optimization predicted from PFV=1.00 calibration data accurately reflects experimental detector performance.

## Workflow Integration and Compliance Considerations

Because this approach relies exclusively on experimentally acquired calibration data, it can be readily implemented within the Empower CDS Software. The workflow supports structured review, traceable documentation, and objective justification of detector settings while maintaining established data integrity expectations (Figure 7). By reducing reliance on repeated experimental recalibration and subjective optimization, this data-driven strategy can improve efficiency during method development while remaining suitable for use in regulated laboratory environments.

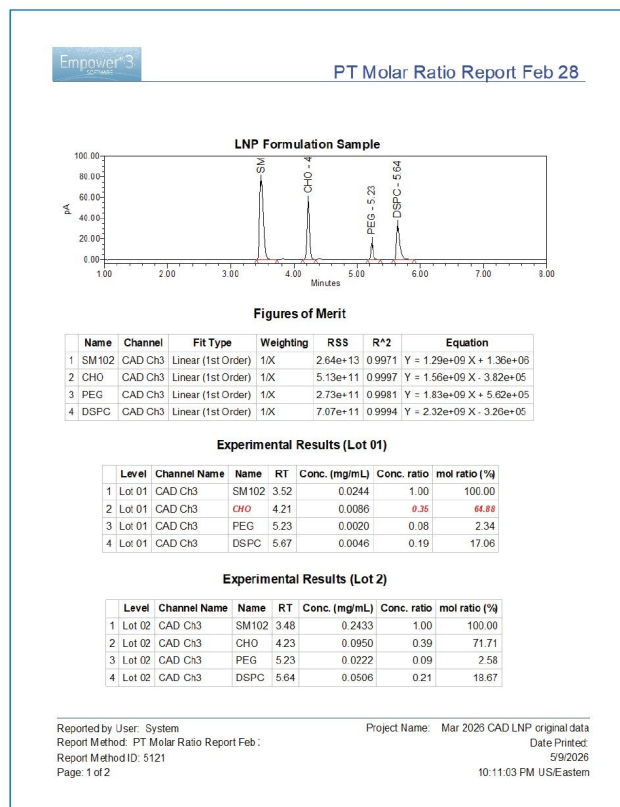
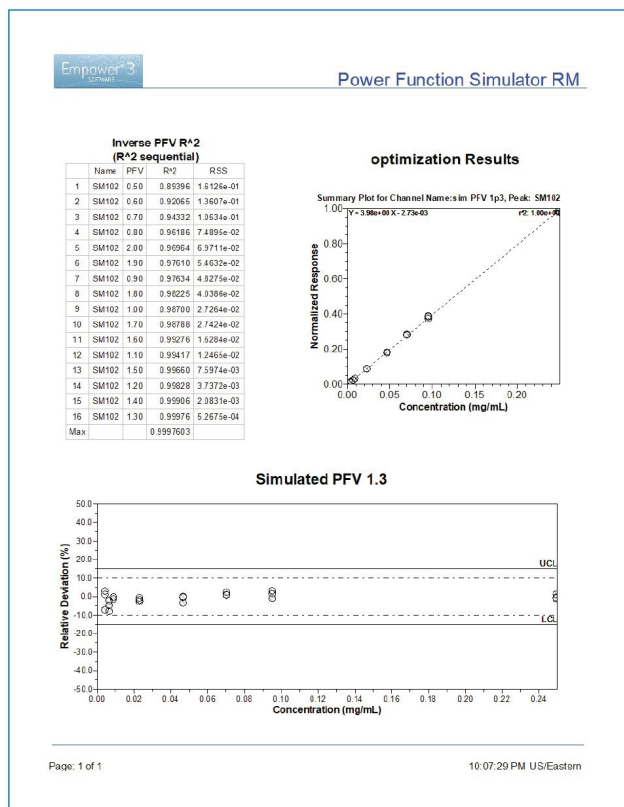


Figure 7. Example workflow illustrating integration of inverse power function modeling within Empower CDS. Calibration data acquired at PFV=1.00 are used for predictive evaluation of PFV settings while maintaining data traceability and auditability for deployment in manufacturing environments.

## Conclusions

- CAD response follows an intrinsic power law relationship that can be characterized using calibration data acquired at PFV=1.00.
- An inverse power function framework enables modeling detector response behavior expediting method development which can reduce experimental burden and operating costs.
- Forward simulation of PFV response allows objective identification of an effective linear operating range, informed by residual behavior and variance rather than correlation metrics alone.

- Integration of experimental variance into the modeling framework supports robust selection of regression weighting strategies and improves quantitative reliability across wide dynamic ranges.
- This data-driven approach enables a transparent and analytical optimization of CAD settings within established chromatography data system workflows.

---

## References

1. Han, D.; DeLaney, K.; Alden, B.; Birdsall, R.; Yu, Y. Lipid Nanoparticle Analysis: Leveraging MS to Reduce Risk. (2022), Waters Application Note. [720007716](#).
2. Fekete, S.; et al. Challenges and emerging trends in liquid chromatography-based analyses of mRNA pharmaceuticals. *J Pharm Biomed Anal.* 2023;224:115174. doi:10.1016/j.jpba.2022.115174.
3. Han, D.; Birdsall, R.; Simeone, J.; Fogwill, M.; Yu, Y. Comparing ELSD and CAD Performance on Polysorbate Quantification in Infliximab Drug Products. (2022), Waters Application Note. [720007501](#).
4. Maziarz, M.; Harden, S.; Rainville, P. Determination of Fatty Acid Composition in Polysorbate 80 using HPLC with Charged Aerosol Detection. (2026), Waters Application Note. [720009340](#).
5. Birdsall, R.; Du, X.; Bigos, P.; Han, D.; Bhiwankar, N. Automating Charged Aerosol Detection (CAD) Analysis with Empower™ CDS Software Using a Single-Vendor Integrated LC Platform. (2026), Waters Application Note. [720009297](#).
6. International Council for Harmonisation of Technical Requirements for Pharmaceuticals for Human Use (ICH). *ICH Q2(R2): Validation of Analytical Procedures*. ICH; 2023.

---

## Featured Products

[ACQUITY Premier System <](#)

<https://www.waters.com/nextgen/global/products/chromatography/chromatography-systems/acquity-premier-system.html>>

[Charged Aerosol Detector <](#)

<https://www.waters.com/nextgen/global/products/chromatography/chromatography-detectors/charged-aerosol-detector.html>>

---

Empower Chromatography Data Software (CDS) <

<https://www.waters.com/nextgen/global/products/informatics-and-software/chromatography-software/empower-software-solutions/empower-cds.html>>

720009440, June 2026



© 2026 Waters Corporation. All Rights Reserved.

[利用規約](#) [プライバシー通知](#) [商標](#) [キャリア](#) [法的通知およびプライバシー通知](#) [Cookies](#) [Cookie](#)  
[環境設定](#) [私の個人情報を販売しないでください](#)